

# Post-translational polymodification of $\beta 1$ tubulin regulates motor protein localisation in platelet production and function

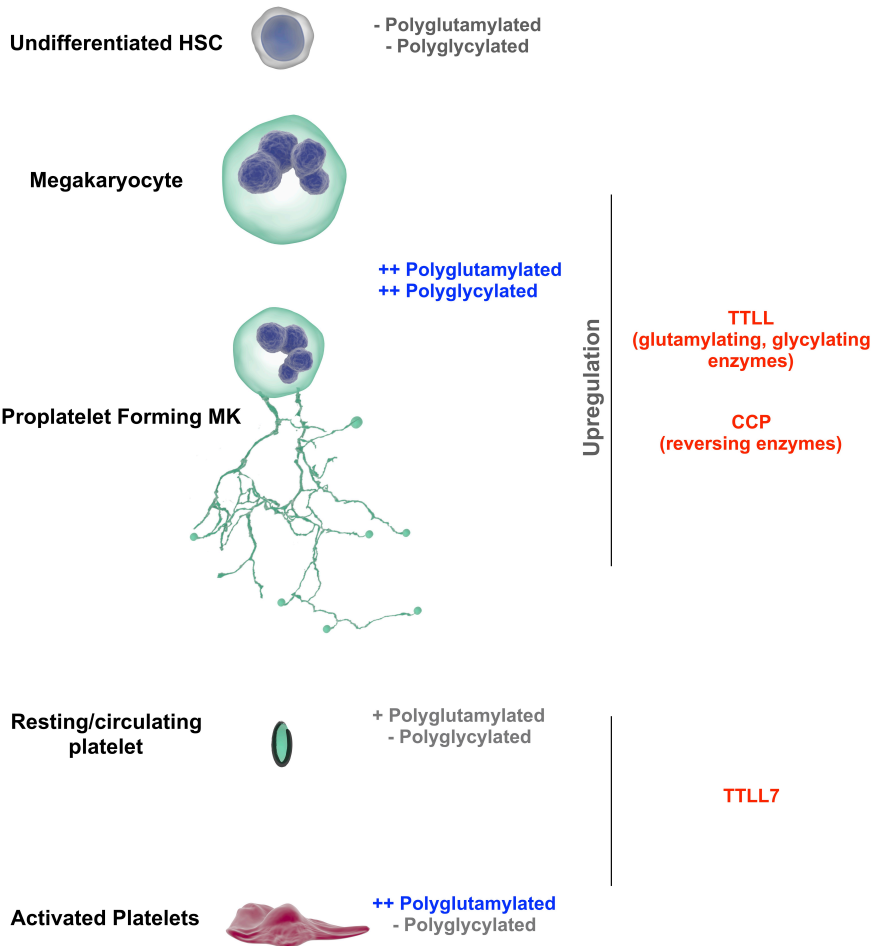
Abdullah O. Khan<sup>1</sup>✉, Alexandre Slater<sup>1</sup>, Annabel MacLachlan<sup>1</sup>, Phillip L.R. Nicolson<sup>1</sup>, Jeremy A. Pike<sup>1,2</sup>, Jasmeet S. Reyat<sup>1</sup>,  
Jack Yule<sup>2</sup>, Steven G. Thomas<sup>1,2</sup>, and Neil V. Morgan<sup>1</sup>✉

<sup>1</sup> Institute of Cardiovascular Sciences, College of Medical and Dental Sciences, University of Birmingham, Edgbaston, Birmingham, UK, B15 2TT

<sup>2</sup> Centre of Membrane and Protein and Receptors (COMPARE), University of Birmingham and University of Nottingham, Midlands, UK

In specialised cells, the expression of specific tubulin isoforms and their subsequent post-translational modifications drive and coordinate unique morphologies and behaviours. The mechanisms by which  $\beta 1$  tubulin, the platelet and megakaryocyte lineage restricted tubulin isoform, drives platelet production and function remains poorly understood. We investigated the roles of two key post-translational polymodifications (polyglutamylation and polyglycation) on these processes using a cohort of thrombocytopenic patients, human induced pluripotent stem cell (iPSC) derived megakaryocytes, and healthy human donor platelets. We find distinct patterns of polymodification in megakaryocytes and platelets, mediated by the cell specific expression of effecting (Tubulin Tyrosine Ligase Like - TTLL) and reversing (Cytosolic Carboxypeptidase - CCP) enzymes. The resulting microtubule patterning spatially regulates motor proteins to drive proplatelet formation in megakaryocytes, and the cytoskeletal reorganisation required for thrombus formation. This work is the first to show a reversible system of polymodification by which different cell specific functions are achieved.

Correspondence: [a.khan.4@bham.ac.uk](mailto:a.khan.4@bham.ac.uk), [N.V.Morgan@bham.ac.uk](mailto:N.V.Morgan@bham.ac.uk). Lead contact: AO Khan. [a.khan.4@bham.ac.uk](mailto:a.khan.4@bham.ac.uk)



## 1 Key Points

- 2 • The platelet specific  $\beta 1$  tubulin (encoded by *TUBB1*) is polyglutamylated and polyglycylated in platelet producing iPSC-  
3 derived megakaryocytes (MKs).
- 4 • The platelet marginal band is polyglutamylated upon activation.
- 5 • Polymodification in both MKs and platelets impact motor protein localisation.
- 6 • Patients with C-terminal *TUBB1* variants demonstrate macrothrombocytopenia, and the CRISPR mediated knock out of  
7 *TUBB1* in iPSC-MKs results in a complete loss of proplatelet production.
- 8 • 3 unrelated families with mutations in *TTLL10* report moderate to severe bleeding and increased mean platelet volume  
9 (MPV), suggesting polyglycation through *TTLL10* is required for healthy platelet production.
- 10 • A system of reversible polymodifications mediated through the graded expression of modifying enzymes (TTLLs and  
11 CCPs) throughout MK maturation is required for proplatelet formation and subsequent platelet function.

## 12 Introduction

13 Microtubules are large, cytoskeletal filaments vital to a host of critical functions including cell division, signalling, cargo  
14 transport, motility, and function(1–3). Despite their ubiquitous expression and high structural conservation, microtubules also  
15 drive unique morphologies and functions in specialist cell types like ciliated cells, spermatozoa, and neurons(4, 5). The question  
16 of how filaments expressed in every cell in the body can facilitate complex and highly unique behaviours like neurotransmitter  
17 release and retinal organisation has been addressed by the *tubulin code*. This is a paradigm which accounts for the specialisation  
18 of microtubules and their organisation by describing a mechanism in which particular cells express lineage restricted isoforms  
19 of tubulin. These cell specific isoforms are then subject to a series of post-translational modifications which alter the mechanical  
20 properties of microtubules, and their capacity to recruit accessory proteins (e.g. motor proteins)(1–3, 5).

21 A host of tubulin post-translational modifications (PTMs) have been reported in a range of cell types, including (but not limited  
22 to) tyrosination, acetylation, glutamylation, glycation, and phosphorylation. In recent years links between the loss of specific  
23 tubulin PTMs, either through the aberrant expression of tubulin isoforms or the loss of effecting or reversing enzymes, has  
24 emerged (5). The loss of post-translationally modified tubulin has been reported to impact motile and non-motile ciliary  
25 function (including respiratory cilia, retinal cells), spermatogenesis, muscular disorders, and neurological development and  
26 function(1, 5–11). Of the many cell systems in which careful regulation of tubulin modification is required for healthy function,  
27 the role of the tubulin code in the generation of blood platelets from their progenitors, megakaryocytes (MKs) remains relatively  
28 poorly understood.

29 Platelets are the smallest component of peripheral blood, and circulate as anucleate cells with an archetypal discoid shape  
30 maintained by a microtubule marginal band(12, 13). The activation of platelets involves a tightly regulated rearrangement of  
31 the cytoskeleton which results in a series of shape changes(13–15). Antagonistic motor proteins maintain the resting state of  
32 the marginal band, and during platelet activation a motor protein dependent mechanism results in sliding which extends the  
33 marginal band and causes the transition to a spherical shape (13, 14). The disc-to-sphere transition is a critical part of platelet  
34 activation, which also involves the secretion of granules as a terminal step in platelet activation.

35 Conversely megakaryocytes are the largest and rarest haematopoietic cell of the bone marrow. These cells are characteristically  
36 large, polyploid cells with unique morphological structures (e.g. the invaginated membrane system (IMS)) required to facilitate  
37 the production of thousands of blood platelets and package within them the required pro-thrombotic factors(16). Extensive  
38 cytoskeletal remodelling is critical to the maturation of MKs and the maintenance of key structures like IMS, as well as to  
39 the production of platelets themselves(15, 16). MKs form long, beaded extensions into the lumen of bone marrow sinusoids -  
40 where these proplatelet extensions then experience fission under the flow of sinusoidal blood vessels which results in the release  
41 of barbell shaped pre-platelets and platelets into the blood stream(16).

42 Both MKs and platelets express a lineage restricted isoform of  $\beta$  tubulin ( $\beta$ 1 tubulin) encoded by the gene *TUBB1*(17). In hu-  
43 mans, *TUBB1* mutations have been shown to result in impaired platelet production, with a resulting macrothrombocytopenia(18,  
44 19). More recently, a C-terminal truncation of  $\beta$ 1 tubulin has been shown to cause a macrothrombocytopenia, suggesting that  
45 C-terminal modifications may be drivers of protein function and causative of the disease phenotype observed (20).  
46 While the loss of *TUBB1* is known to result in macrothrombocytopenia, the mechanisms by which this isoform of tubulin effects  
47 the dramatically different cytoskeletal behaviours of platelets and MKs remains poorly understood. In the context of the tubulin  
48 code, MKs and platelets present a particularly interesting model. Both cells express a specific  $\beta$  tubulin isoform ( $\beta$ 1 encoded  
49 by *TUBB1*), but undergo markedly different cytoskeletal changes. To date, acetylation and tyrosination have been the PTMs  
50 primarily reported in MKs and platelets, however neither modification is specific to the C-terminal tail encoded by *TUBB1*.  
51 Fiore *et al.* show that a C-terminal truncation of *TUBB1* phenocopies the complete loss of the protein(13, 21). We therefore hy-  
52 pothesise that PTMs specific to the C-terminus of *TUBB1* are required for the complex morphological rearrangements required  
53 for both MK and platelet function.  
54 The C-terminal tail of  $\beta$ 1 tubulin is particularly rich in glutamate residues which are often targeted for two key post-translational  
55 modifications implicated in human disease. Polyglutamylation and glycation are PTMs which target glutamate residues on  
56 both tubulin subunits ( $\alpha$  and  $\beta$ ) and result in the addition of glutamate or glycine residues respectively(1, 2, 22). Interestingly  
57 polyglutamylation has been observed in microtubules in centrioles, axenomes, neuronal outgrowths, and mitotic spindles(1, 2).  
58 Thus far polyglycation has primarily been observed in axenomes, suggesting a role for polyglycation and polyglutamylation  
59 in regulating ciliary function - with important consequences for ciliopathies(1). As these polymodifications target the same  
60 substrate, namely glutamate residues in tubulin tails, it has been suggested that these PTMs are competitive. For example,  
61 glutamylation is evident on  $\beta$  tubulin in post-natal development, but is found on  $\alpha$ -tubulin in younger neurons(23). There is  
62 some debate as to whether these polymodifications negatively regulate one another(24, 25). Mutations in the glutamylases  
63 and deglutamylases regulating polymodification can cause male infertility through aberrant spermatogenesis and poor sperm  
64 motility, as well as dysfunctions in airway cilia and axonal transport (9, 11, 26–29).  
65 To date polyglycation has not been reported in MKs or platelets. Recently Van Dijke *et al.* reported on the polyglutamylation  
66 of  $\beta$ 1 tubulin in a CHO cell line engineered to express *TUBB1* downstream of the integrin  $\alpha_2\beta_3$ , and platelets spread on  
67 fibrinogen(30). However, to effectively study and interpret the effects of post-translationally modified tubulin residues a model  
68 is required which recapitulates the complex network of regulatory enzymes effecting and reversing PTMs. This is particularly  
69 important in light of potential evolutionary divergences in the function of TTLL enzymes implicated by Rogowski *et al.*(25).  
70 To interrogate the polymodification of the C-terminal tail of *TUBB1* as a driver of both platelet formation and function, we  
71 report on two unrelated families with variants in the C-terminal region of *TUBB1* gene, resulting in a macrothrombocytopenia  
72 and bleeding. Existing cell lines poorly emulate the expression profiles and platelet producing capacity of MKs, therefore  
73 to develop a representative model we adapt a directed differentiation protocol to generate a large population of proplatelet  
74 forming MKs from induced pluripotent stem cells (iPSCs), and apply these cells to report on the extensive polyglycation and  
75 polyglutamylation of proplatelet forming MKs. We demonstrate that these polymodifications are removed in resting platelets,  
76 but that upon activation, platelets undergo a specific polyglutamylation of the marginal band to undergo spreading.  
77 We go on to show that on platelet activation, kinesin and dynein poorly co-localise with polyglutamylated residues, supporting  
78 previous work which suggests that polyglutamylation impacts motor protein processivity. We therefore reason that polyglu-  
79 tamylation is the mechanism by which platelet marginal bands are destabilised on activation. The role of polyglycation in  
80 platelet activity remains unclear, however we report on patient variants in 3 unrelated families which result in a loss-of-function  
81 of the polyglycylase *TTLL10*, suggesting a role for this gene, previously thought to be non-functional in humans, in platelet  
82 production.  
83 Finally, we perform a quantitative mRNA-expression analysis of the 13 known mammalian tubulin tyrosin like ligases (TTLLs)  
84 and 6 Cytosolic Carboxypeptidases (CCPs) and report an increase in the expression of specific TTLLs and CCPs in maturing  
85 and proplatelet forming MKs. Our *in vitro* work identifies a mechanism by which maturing MKs express a palette of TTLLs  
86 and CCPs to reversibly polyglutamylate and polyglycylate  $\beta$ 1 tubulin to regulate motor protein motility and drive platelet  
87 production. Knocking-out *TUBB1* in iPSC-MKs results in a loss of platelet production, and disordered polymodification.

88 In platelets a single polyglutamylase, TTLL7 is expressed to drive the polyglutamylation of the marginal band needed to  
 89 destabilise this structure for platelet activation and shape change. This study reports on a highly unique mechanism of reversible  
 90 post-modification which drives the specialist behaviours of both platelets and their progenitors, MKs.

## 91 Results

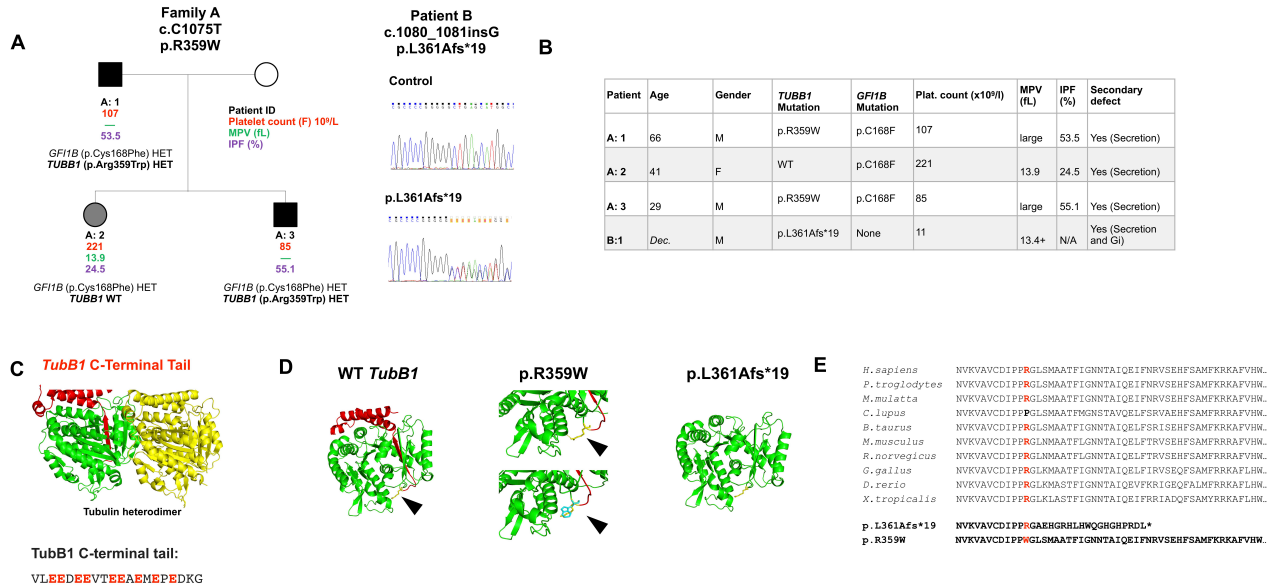


**Fig. 1. Candidate *TUBB1* mutations and their hypothesised effect on the C-terminus of  $\beta 1$  tubulin.** (A,B) Two unrelated families were identified as carrying mutations in the *TUBB1* gene within 6 base pairs of one another. The first, family A, is comprised of 3 individuals, two of whom carry an Arginine to Tryptophan (p.R359W) coding mutation. Interestingly, all 3 individuals in family A harbour a *GF1B* mutation. However, the individuals with the reported *TUBB1* mutation (A:1 and A:3) present with a macrothrombocytopenia and high IPF, while the patient without the R359W *TUBB1* mutation presented with a normal platelet count. The second family is comprised of a single individual, recently deceased, with a frameshift mutation 6 base pairs from the missense reported in family A. In this individual's case, the insertion of a guanine nucleotide results in a frameshift with a premature stop codon 19 amino acids from the leucine to alanine change. (C) The C-terminal tail is downstream of both mutations in these families, and projects away from the dimer:dimer interface. The C-terminal sequence of *TUBB1* is rich in glutamate residues which can be targeted for post-modification. (D) Based on homology modelling of *TUBB1*, we predict that the missense mutation reported in family A is likely to affect the fold of the C-terminal tail, while the frameshift causes a truncation of this region. (E) The arginine residue mutated in family A is highly conserved across species, as are sequences adjacent to the frameshift in patient B.

**92 Identification and initial characterisation of *TUBB1* variants in patients with inherited thrombocytopenia and**  
**93 platelet dysfunction.** Using whole exome sequencing of patients recruited to the GAPP (Genotyping and Phenotyping of  
**94 Platelets) study, two C-terminal *TUBB1* variants were identified in unrelated families presenting with macrothrombocytopenia**  
**95 (Figure 1 A).** Affected individuals in Family A were found to be heterozygous for a C>T transition resulting in an arginine  
**96 to tryptophan amino acid substitution (c.C1075T, p.R359W) in *TUBB1*.** Individuals in this family also carry a *GF1B* variant  
**97 (p.Cys168Phe).** Variants in both genes have been linked to thrombocytopenia, however only individuals A:1 and A:3, both  
**98 of whom carry *TUBB1* variants, present with a macrothrombocytopenia ( $107$  and  $85 \times 10^9/L$  respectively).** Individual A:2  
**99 carries the *GF1B* variant but is wild type for *TUBB1* and presents with a normal platelet count ( $221 \times 10^9/L$ ).** This shows that  
**100 the *TUBB1* variant is responsible for the macrothrombocytopenia, and not *GF1B*.** Interestingly, individuals A:1 and A:3 also  
**101 present with significantly higher immature platelet fractions (IPFs) and mean platelet volumes (MPVs) when compared to their**  
**102 *TUBB1* WT relative (53.5% and 55.1% compared to 25.5%, MPV for A:1 and A:3 too large for measurement).** This variation  
**103 in count and phenotype suggest that *TUBB1* is causative of the macrothrombocytopenia observed.**  
**104 Family/patient B was an elderly gentleman (now deceased) with a G insertion and subsequent frameshift truncation of the pro-**  
**105 tein 19 amino acids from the site of insertion (c.1080insG, p.L:361Afs\*19).** This patient had a severe macrothrombocytopenia  
**106 with a platelet count of  $11 \times 10^9/L$  and an MPV above  $13.4$  (Figure 1B).** At the time of study, IPF measurement was unavailable.  
**107 Both *TUBB1* variants are positioned in the C-terminal region of the  $\beta 1$  isoform encoded by *TUBB1* as indicated in figures**  
**108 1 C and D.** This region is positioned away from the dimer:dimer interface, and the C-terminal tail is an established site for  
**109 post-translational modification (PTM), particularly as it is rich in glutamate residues which are known targets for glutamyl-**

110 and glycation (1)(Figure 1 C,D). Both affected *TUBB1* sequence variants are highly conserved in mammals (Figure 1 E). We  
111 predicted that the R359W missense substitution is likely to alter the folding of the C-terminal tail, potentially affecting PTM  
112 or interactions with critical microtubule accessory proteins (MAPs) (Figure 1 C,D). Similarly the G insertion and subsequent  
113 frameshift are likely to truncate the C-terminal region.

114 Patient platelet function was investigated using flow cytometry due to the reduced platelet count observed. Patient B demon-  
115 strated a significant reduction in surface P-selectin and fibrinogen uptake in response to all agonists tested(Figure S1). Family  
116 A showed no change in the levels of surface receptor expression, but showed weak P-selectin and fibrinogen responses when  
117 activated with a low concentration ADP, CRP, and PAR-1, suggesting a mild secretion defect (Figure S1 C,D).

118 Patients with C-terminal variants in this study and others previously reported by Fiore *et al.* phenocopy individuals with a  
119 complete loss of the  $\beta$ 1 tubulin (18–20), suggesting that the C-terminal tail is likely critical to the function of *TUBB1* in the  
120 myriad complex roles of microtubules in both MKs and platelets. As this C-terminal tail is rich in glutamate residues which are  
121 often targeted for polymodification, we began to investigate the role of polyglutamylation and polyglycylation in human stem  
122 cell derived megakaryocytes and healthy donor platelets.

123 **iPSC-derived proplatelet forming MKs are both polyglycylated and polyglutamylated.** Polyglutamylation has recently  
124 been reported in a modified CHO cell line and human platelets, however no evidence of this PTM has been reported in human  
125 MKs. A species dependent variation in the expression of modifying enzymes has been reported and discussed, therefore a  
126 human model is required to investigate the role of this polymodification in platelet production (25, 30, 31). To date, polyg-  
127 lycylation has not been reported in either platelets or megakaryocytes, however both modifications target the same glutamate  
128 residues, suggesting a potentially competitive mechanism by which these PTMs are applied to  $\beta$ 1 tubulin.

129 To investigate polymodification in human megakaryocytes, we adapted a directed differentiation protocol previously reported  
130 by Feng *et al.* to generate large populations of mature, proplatelet forming cells (Supplementary Figure S2). Cells were  
131 differentiated and stained for CD42b as a marker for mature, and hence *TUBB1* expressing, MKs, and both polyglutamylated  
132 and polyglycylated tubulin. CD42b positive cells, including proplatelet forming cells, were also found to be positive for  
133 both polyglutamylated tubulin and polyglycylated tubulin (Figure 2 A,B), while neighbouring cells in the sample negative for  
134 CD42b did not demonstrate these polymodifications (Figure 2 C). Across multiple differentiations we consistently yielded a  
135 purity of approximately 50-60% CD42b positive cells (Figure 2 D), which on analysis are positive for both polyglutamylated  
136 and polyglycylated tubulin (Figure 2 E). Finally, 100% of proplatelet forming cells observed across replicates were positive for  
137 both polyglutamylated and polyglycylated tubulin (Figure 2 F). The presence of polyglutamylated and polyglycylated tubulin  
138 in these samples was further confirmed through western blotting of mature iPSC lysate from three independent differentiations  
139 (Figure 2G).

140 **A. CRISPR knock-out of *TUBB1* results in a complete loss of proplatelet formation.** To date, the loss of *TUBB1* has not  
141 been studied in human MKs. To interrogate the loss of the protein and its post-translational modifications, we generated an iPSC  
142 line with bi-allelic loss of function mutations in the N-terminus of the coding region of *TUBB1* (Figure 2 H, Supplementary  
143 Figure S3). Loss of the *TUBB1* start codon on both alleles results in a loss of protein expression (Figure 2 I), and a complete  
144 loss of platelet production *in vitro* (Figure 2 J,K). This is identical to homozygous murine knock-outs (17).

145 Interestingly while *TUBB1* knock-out clones stain positively for polyglutamylated and polyglycylated tubulin, the distribution  
146 of these residues is disturbed when compared to wild type platelet forming iPSC-MKs (Figure 2 L). While polyglycylated and  
147 polyglutamylated residues form a distinct peripheral band around wild type MKs as shown in colourised Z-stacks in figure 2 L,  
148 the knock-out cells appear to have a disordered pattern.

149 **Platelet activation results in the polyglutamylation of the marginal band.** MKs and platelets both achieve markedly  
150 different morphologies and functions despite the expression of *TUBB1* in both cell types. As such we hypothesized that the  
151 *TUBB1* polymodifications evident in MKs might be differently regulated between resting and activated platelets. We therefore  
152 compared immunofluorescence staining of polyglutamylated and polyglycylated tubulin between resting platelets and cells  
153 spread on fibrinogen and collagen. We found that resting platelets demonstrate a diffuse distribution of polyglutamylated

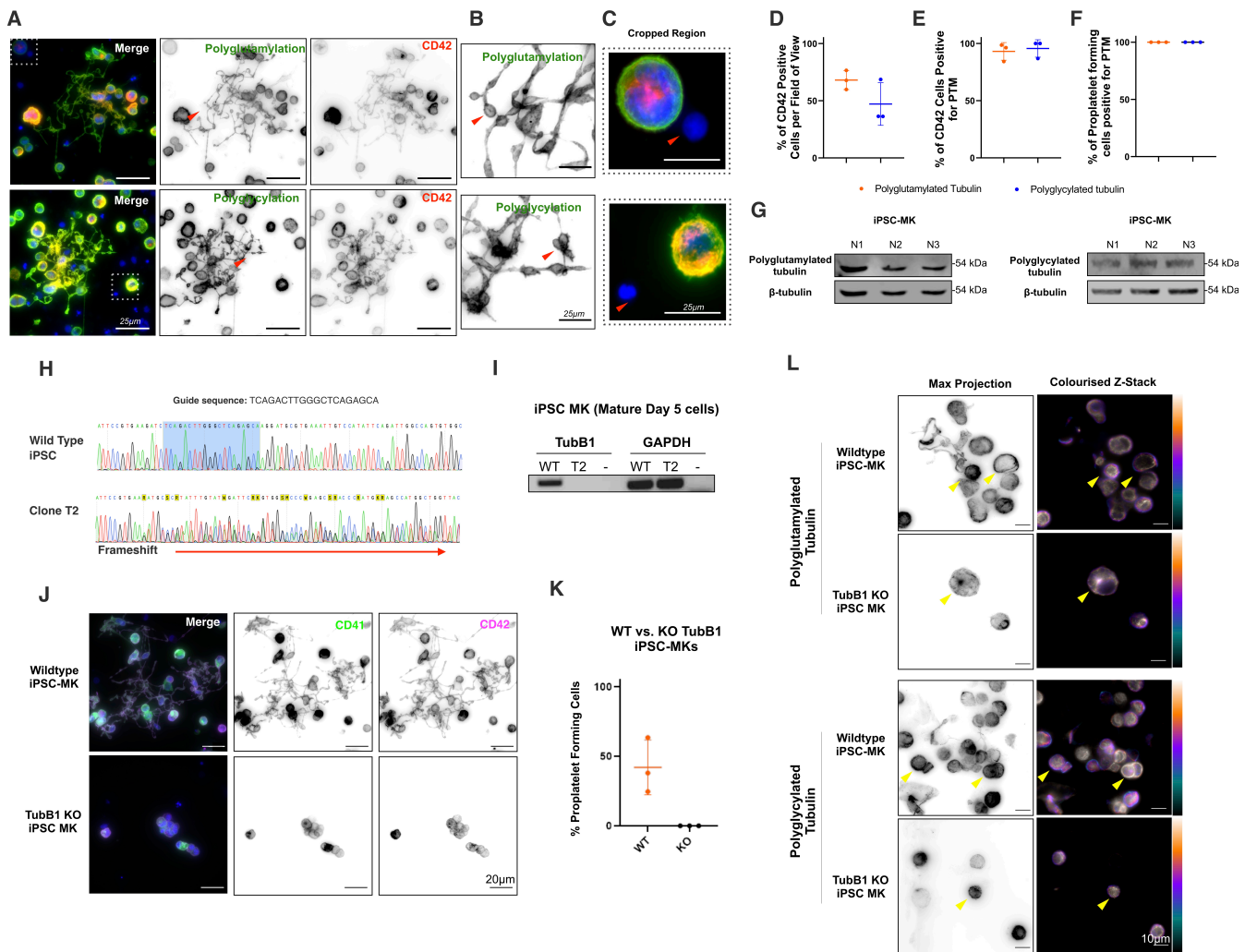


**Fig. 2. Mature, proplatelet forming iPSC-MKs are both polyglutamylated and polyglycylated. TubB1 knock-out iPSC-MKs do not form proplatelets and demonstrate disordered polymodified tubulin.** (A) iPSC-MKs co-stained for CD42 and polyglutylated or polyglutamylated tubulin show that these cells are positive for both polymodifications. (B) Both polyglutamylated and polyglycylated tubulin are evident in proplatelet extensions, including nascent platelet swellings on the proplatelet shaft (indicated by red arrows). (C) Neighbouring CD42b- cells are also negative for both polymodifications. (D, E) Approximately 50-60% of cells in multiple differentiations are positive for CD42b, and these cells are 100% double positive for polymodification and CD42b. (F) All proplatelet extensions observed are positive for polymodification. (G) Polyglutamylation and polyglycation are evident by western blotting in mature iPSC-MKs. (H) iPSC were transfected with a *TUBB1* targeting guide RNA, after which indel positive cells were isolated and sequenced to positively identify a bi-allelic insertion-deletion mutant (clone T2). (I) This clone was further analyzed and loss of  $\beta$ 1 tubulin expression was confirmed by qRT-PCR. (J,K) A comparison of proplatelet production in wild-type vs. *TUBB1* KO cells revealed a reduction in the number of CD41/42b+ cells in the knock-out clone, and a complete loss of proplatelet formation in mutant clones. (L) *TUBB1* knock-out clones show a disordered arrangement of polymodified residues when compared to wild type cells. Colourised Z-stacks show a distinctive peripheral band in wild type cells which is lost in the knock-out. ( $n = 3$  independent differentiations, S.D. plotted on graphs)

154 tubulin which partially co-localises with the  $\beta$  tubulin marginal band. Interestingly however, we see a marked increase in the  
 155 polyglutamylation of the marginal band on platelet activation and spreading on fibrinogen (\*\*\*\*  $p < 0.0001$ , \*\*\*  $p 0.003$ )  
 156 (Figure 3 A). Unlike MKs which demonstrate extensive polyglycation in proplatelet forming cells, platelets do not have  
 157 polyglycylated tubulin. (Figure 3 B).

158 Western blotting of resting platelets and cells activated through exposure to CRP over time does not show an increase in the total  
 159 amount of polyglutamylated tubulin in the sample (Figure 3C). Interestingly, analysis of the co-localisation between  $\beta$  tubulin  
 160 and polymodified residues shows a significant increase in co-localisation between polyglutamylated tubulin and the marginal  
 161 band in both fibrinogen and collagen spread cells. No significant change in co-localisation is observed for polyglycylated  
 162 residues (Figure 3 D).

163 To investigate the distribution of both polyglutamylated and polyglycylated tubulin in the context of thrombi, platelets were  
 164 activated *in vitro* using CRP and subsequently fixed and mounted on to Poly-L-Lysine coated coverslips. These cells were then

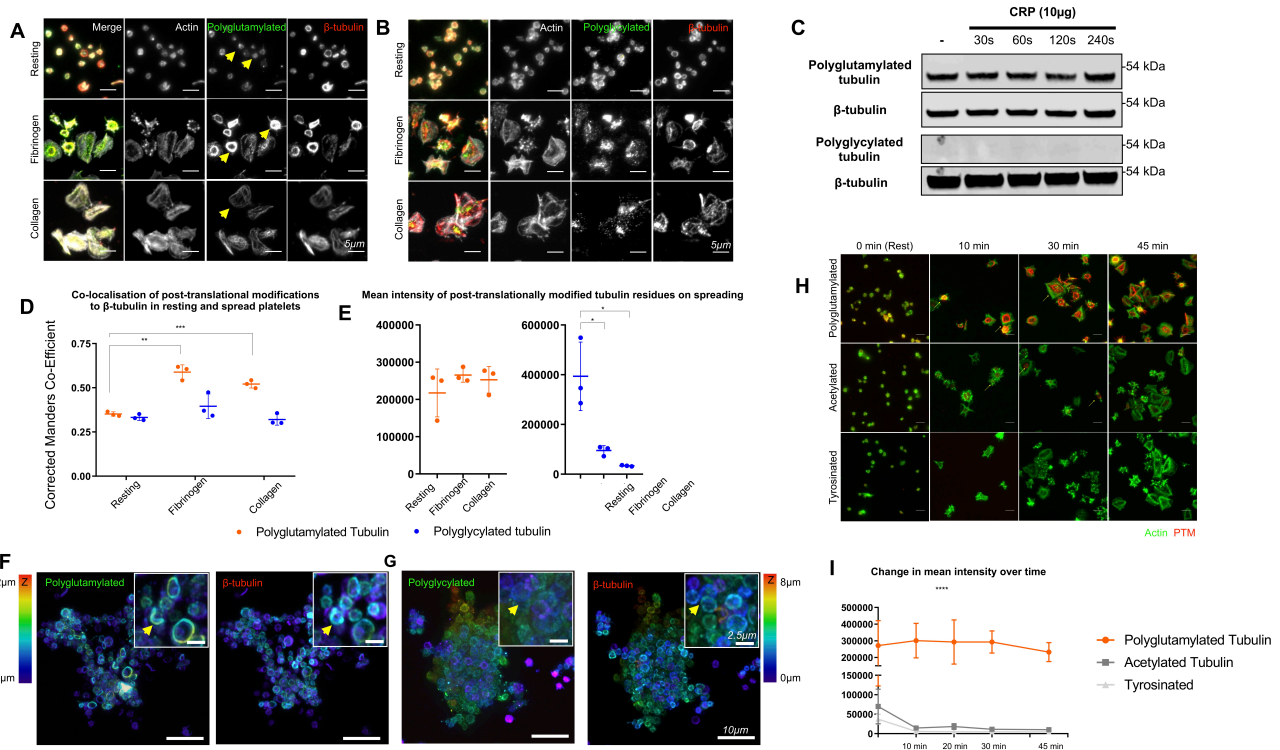


**Fig. 3. Platelet activation results in polyglutamylation of the marginal band** (A) Resting platelets show a diffuse distribution of polyglutamylated tubulin which partially co-localises with the marginal band (yellow arrows), however, on spreading on fibrinogen, a marked increase in the polyglutamylation of the marginal band is observed (yellow arrows). (B) Tubulin in platelets is not consistently polyglycylated. (C) Western blotting of resting and CRP activated platelets confirms the presence of polyglutamylated tubulin and a loss of polyglycylation. (D) A measurement of co-localisation (corrected Manders coefficient) between polyglutamylated tubulin and  $\beta$  tubulin in resting and spread platelets shows a significant increase in the co-localisation of these modified tubulin residues on platelet activation and spreading. This change localisation is not observed between polyglycylated residues and  $\beta$  tubulin. (E) Measurements of fluorescence mean intensity in polyglutamylated and polyglycylated tubulin shows a change in polyglutamylated tubulin consistent with western blotting, and a decrease in polyglycylated tubulin. (F) Platelets activated *in vitro* using Collagen Related Peptide (CRP) were co-stained for  $\beta$  tubulin and polyglutamylated residues and imaged in 3D using AiryScan confocal (stacks coloured in Z as indicated by the colour chart in this figure). In these micro-thrombi, extensive polyglutamylation of the marginal band is evident. (G) Similar samples stained for polyglycylated residues do not consistently label tubulin. (H) A time course was performed to compare polyglutamylated tubulin with two other previously reported PTMs in platelets (acetylation and tyrosination). No significant acetylation or tyrosination of the marginal band is evident over a 45 minute time course, however polyglutamylation of the marginal band is evident throughout the time course. (I) The mean fluorescence intensity of polyglutamylated tubulin is markedly higher than either acetylated or tyrosinated tubulin. ( $n = 3$ , S.D., Two-Way ANOVA with multiple comparisons. 10  $\mu$ m scale bar.)

165 stained for both  $\beta$  tubulin and polyglutamylated or polyglycylated tubulin respectively (Figure 3 F,G). Interestingly, polyglu-  
 166 tamylated tubulin is evident throughout the aggregate on the marginal band of platelets, while polyglycylated tubulin is diffusely  
 167 distributed (Figure 3 F,G). This data shows that while polyglutamylation and polyglycation are evident in platelet producing  
 168 iPSC-MKs, only polyglutamylation is evident in platelets. While the total amount of polyglutamylated tubulin does not change  
 169 on platelet activation, the localisation of these residues changes dramatically, suggesting that polyglutamylation of the marginal  
 170 band specifically is key to the reorganisation of the microtubule cytoskeleton required for platelet function.  
 171 Acetylation and tyrosination have been previously reported in platelets, however their role in maintaining the marginal band  
 172 and/or driving morphological change on platelet activation remains unclear(13). To determine whether the polyglutamylation  
 173 of the marginal band we observe thus far coincides with these PTMs, we performed a time course of spreading on fibrinogen  
 174 to determine whether there is an equivalent increase in either acetylation or tyrosination of the marginal band. Interestingly,  
 175 we find no marked acetylation or tyrosination of this structure over the time course, while a notable polyglutamylation of the  
 176 marginal band is evident from the earliest time point (10 minutes spreading on fibrinogen) (Figure 3 H, I).

177 **MK and platelet polymodification is regulated through the expression of both modifying and reversing enzymes.**  
 178 Thus far we have reported a mechanism by which polyglutamylation and polyglycation occur in mature and proplatelet forming  
 179 MKs, followed by a change in distribution of these polymodifications (a reduction in polyglycation) in the resting platelet,  
 180 and finally an increase in the polyglutamylation of the marginal band on platelet activation and spreading. We hypothesise that

181 the expression of cell specific subsets of effecting (TTLL) and reversing (CCP) enzymes are required to achieve the observed  
182 regulation of these polymodifications.

183 We designed a qRT-PCR panel to interrogate the expression of the 13 known mammalian TTLLs and 6 CCPs. We generated  
184 RNA from iPSC-MKs at different stages of the final terminal differentiation (Figures 4 A, S2A). Day 1 (d1) cells are repre-  
185 sentative of a pool of haematopoietic stem cells (HSCs) and MK progenitors, while day 5 (d5) cells are comprised of 60%  
186 CD41/42b+ cells (Figures 4 A, S2 E). Finally, day 5 cells treated with heparin to induce proplatelet formation (d5 + Hep) were  
187 used to interrogate whether there is any specific up-regulation of TTLLs and/or CCPs on proplatelet formation (Figures 4 A,  
188 S2 D).

189 GAPDH housekeeping controls for each of the 3 samples (d1, d5, d5+Hep) show equivalent amplification of the housekeeping  
190 control, while results for TTLL family proteins show a number of enzymes expressed at different levels across the maturation  
191 of these cells (Figure 4 B,C). Candidate TTLLs observed in the initial endpoint PCR were taken forward for quantification  
192 across replicates generated from multiple differentiations, which included TTLLs 1, 2, 3, 4, 5, 6, 7, 10, and 13 (Figure 4 C,D).  
193 We find a significantly increased expression of TTLL1, TTLL2, TTLL4, and TTLL10 on proplatelet formation in cells treated  
194 with heparin (\*\* p = 0.0081, \* p = 0.0105, \* p = 0.0260, \*\*\* p = 0.0004 respectively) (Figure 4 D).

195 CCP family enzymes were also found to be expressed in maturing MKs, notably CCP1, 3, 4, 5, and 6 (Figure 4 E). Quantifi-  
196 cation across replicates revealed that CCP4 and 6 are up-regulated on proplatelet production (\* p = 0.0130, \*\*\* p = 0.0009)  
197 (Figure 4 F).

198 To determine whether platelets demonstrate a difference in TTLL and CCP expression we repeated the qRT-PCR panel per-  
199 formed on maturing iPSC-MKs on platelet samples from 3 healthy donors. Each donor's platelets were either lysed in the  
200 resting state for RNA, or treated with CRP for 3 minutes to determine if there are changes in expression as a result of platelet  
201 activation. Interestingly, we found that none of the TTLLs and CCPs observed in iPSC MKs were consistently expressed across  
202 donors with the exception of TTLL7, a known polyglutamylase (Figure 4 I, complete gel in figure S7). No differences between  
203 resting and activated platelets were observed (Figure 4 I). This data shows a markedly different pattern of TTLL and CCP  
204 expression in both MKs and platelets, which correlates to the observed differences in polymodification.

205 **TTLL10 variants cause higher MPV and moderate to severe bleeding in 3 unrelated families.** Our qRT-PCR screen  
206 reveals that a number of TTLL and CCPs are up-regulated during the process of platelet production, including the monogly-  
207 cylase TTLL3 and the polyglycylase TTLL10. Three separate families were identified within the GAPP patient cohort with  
208 rare variants in the *TTLL10* gene (Figure 4J). Two of the three variants result in frameshifts towards the N-terminus of the pro-  
209 tein, preceding the ATP binding region (p.Pro15Argfs\*38 and p.Val249Glyfs\*57) (Figure 4J). The final family has a missense  
210 p.Arg340Trp variant.

211 All three families report similar phenotypes, namely normal platelet counts, aggregation and secretion, but consistently high  
212 MPVs (normal ranges Mean Platelet Volume (fL) (7.83-10.5) and an established history of moderate to severe bleeding, in-  
213 cluding cutaneous bruising and menorrhagia (Figure 4K). Interestingly, one of the patients (A 1:1) was further studied, and on  
214 platelet spreading on fibrinogen we observe a marked increase in platelet area compared to controls (Figure 4L).

215 **Platelet and MK polymodifications regulate motor protein localisation to drive both proplatelet formation and**  
216 **platelet shape change on activation.** Thus far we have observed a markedly different distribution of polyglutamylated and  
217 polyglycylated residues in both human iPSC-derived MKs and human donor peripheral blood platelets. Polyglutamylation has  
218 been reported as a means by which motor protein processivity is regulated, and like in neuronal cells, MK proplatelet formation  
219 is known to be driven by a mechanism of dynein mediated proplatelet sliding (32). Similarly, the antagonistic movement of  
220 dynein and kinesin are known to maintain the marginal band in resting platelets(13).

221 We hypothesised that polyglutamylation in both MKs and platelets increases motor protein processivity and therefore alters  
222 the localisation of these proteins. Therefore the polyglycylation evident in MKs (but notably absent in platelets) is likely a  
223 mechanism of regulating motor protein motility to prevent excessive polyglutamylation and control the microtubule sliding  
224 required for platelet production. Interestingly, the polyglutamylation and polyglycylation of proplatelet extensions is analogous

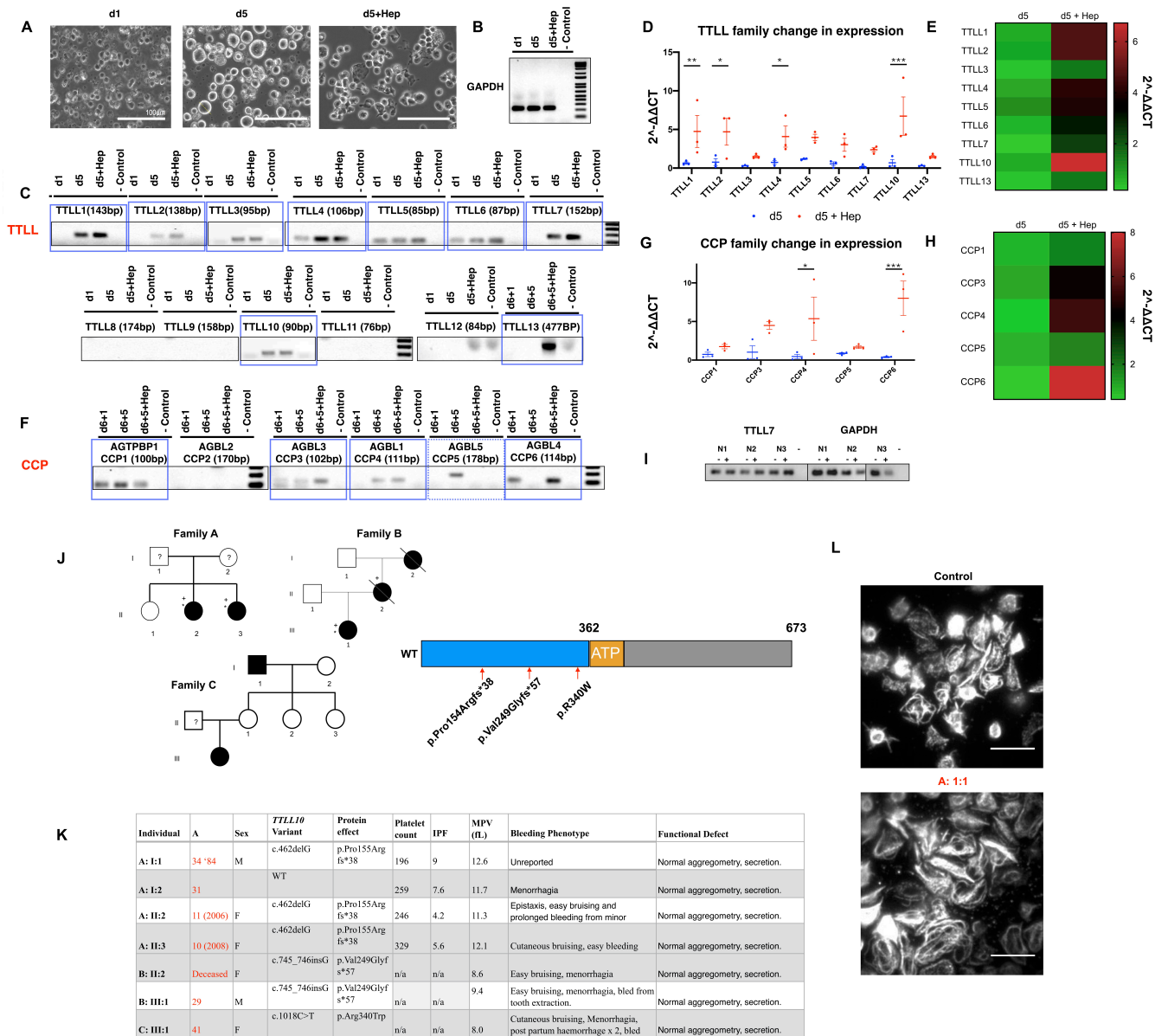


**Fig. 4. iPSC-MKs and platelets differentially express TTLL and CCP enzymes to regulate polymodifications during MK maturation and platelet production. The loss of TTLL10 results in a bleeding phenotype in unrelated human patients.** (A) RNA was generated from iPSC-MKs at different stages of terminal differentiation. Day 1 (d1) cells are comprised of HSCs and progenitors, while day 5 (d5) cells are primarily mature CD41/CD42b double positive cells. Finally, day 5 cells treated with heparin to induce proplatelet formation (d5 + Hep) were used to determine whether an upregulation of these enzymes is evident on platelet production. (B) Samples were amplified with housekeeping GAPDH primers to ensure that any differences in TTLL or CCP expression observed were not due to differences in RNA abundance or quality. (C) A number of TTLL family enzymes were observed, including TTLLs 1, 2, 3, 4, 5, 6, 7, 10, and 13. Of these, a number appeared to be up-regulated in mature and proplatelet forming cells. (D) These samples were taken forward and expression was quantified over multiple differentiations using the  $\delta\Delta CT$  method using d1 cells as controls to determine if there was any upregulation in TTLL expression on platelet production. TTLL 1, 2, 4, and 10 expression was found to be significantly upregulated on treatment with heparin (\*\*  $p = 0.0081$ , \*  $p = 0.0105$ , \*  $p = 0.0260$ , \*\*\*  $p = 0.0004$  respectively). (E) A similar panel was performed on CCP enzymes which reverse polymodifications, with expression of CCP1, 3, 4, 5, and 6 was observed. (F) Statistically significant upregulation of CCPs 4, and 6 were observed on proplatelet production (\*  $p = 0.0130$ , \*\*\*  $p = 0.0009$ ). (G) In resting (-) and CRP activated (+) platelets from 3 healthy donors TTLL7 was the only modifying enzyme found to be consistently expressed. (J) Three unrelated families were identified within the GAPP cohort, two with frameshift truncations and one with a missense (p.Pro155Argfs\*38, p.Val249Glyfs\*57, and p.Arg340Trp respectively). (K) All three families present with normal platelet counts and function, but demonstrate an elevated mean platelet volume (MPV) and consistent histories of bleeding including cutaneous bruising and menorrhagia. (L) Patient A:1:1 volunteered to return and demonstrated abnormally large platelets on spreading on fibrinogen (tubulin staining, 10  $\mu$ m scale bar). (n = 3, S.D., Two-Way ANOVA with multiple comparisons performed. Complete unedited gels found in figures S6,S7.)

to the polymodifications observed in ciliated cells, suggesting a potential role for axonemal dyneins in facilitating these unique cellular processes.

To test this hypothesis, we first performed a time course of platelet spreading on fibrinogen and measured co-localisation between polyglutamylated tubulin and axonemal dynein (DNAL1 - axonemal light chain 1). We observe a sharp loss of co-

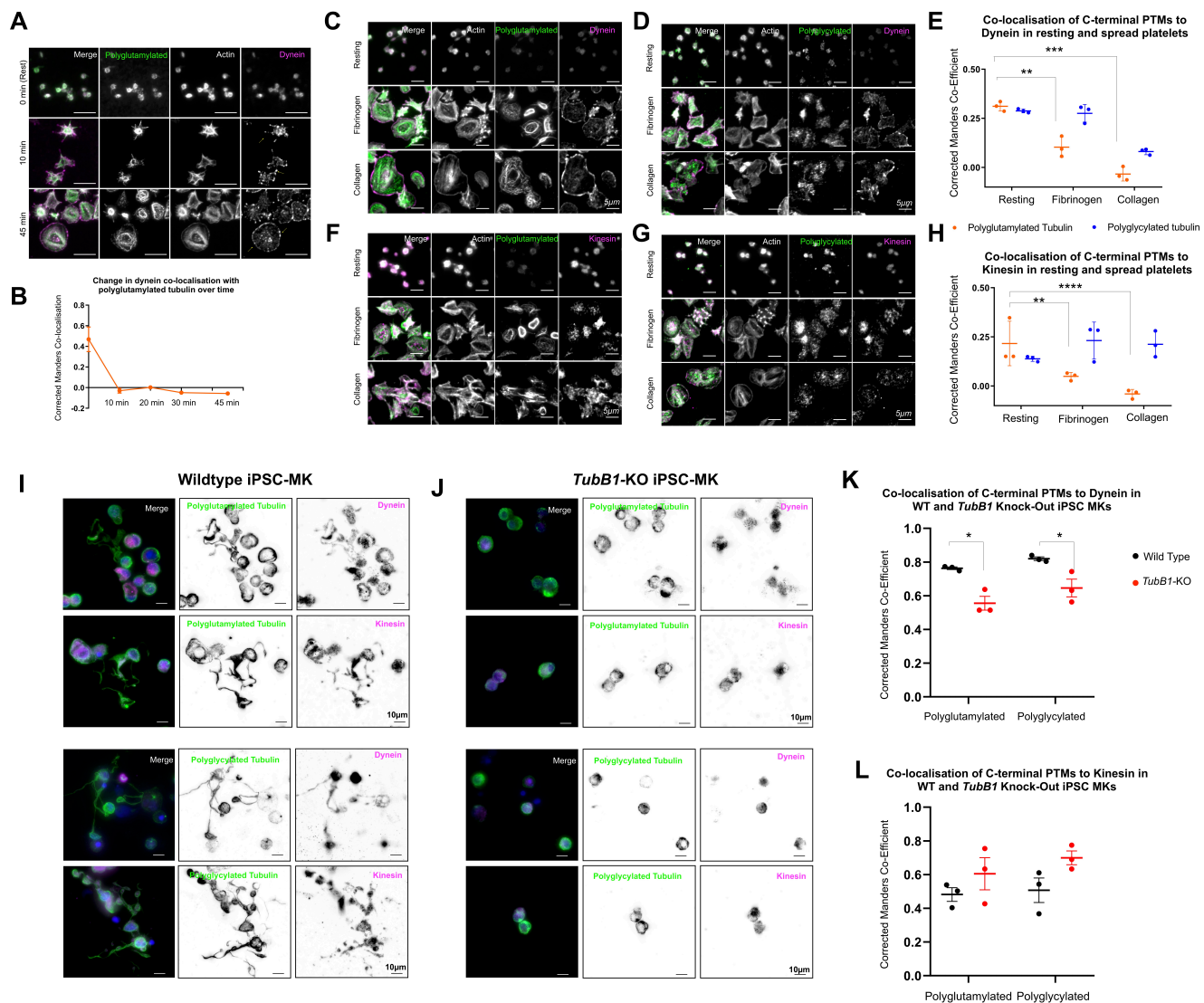


**Fig. 5. Polyglutamylation regulates spatial distribution of motor proteins in platelets and MKs.** (A, B) Quantification of the co-localisation of dynein, as measured by the corrected Manders coefficient, with polyglutamylated tubulin over time shows a marked decrease in co-localisation on platelet activation. (C,D) In fibrinogen and collagen spread cells, axonemal dynein is observed on the periphery of the cell with no particular co-localisation evident with either polyglutamylated or polyglycylated tubulin. (E) Dynein co-localisation with polyglutamylated residues decreases dramatically on platelet spreading in both fibrinogen and collagen (\*\*  $p = 0.0082$  and  $p = *** 0.0004$  respectively). No significant change in co-localisation with polyglycylated residues is observed. (F,G) Kinesin-1 staining is more diffuse throughout resting and spread platelets, on quantification (H) a loss of co-localisation with polyglutamylated tubulin is evident in fibrinogen and collagen spread cells (\*\*  $p = 0.0017$ , \*\*\*\*  $p < 0.0001$  respectively), with no significant change in co-localisation with polyglycylated tubulin. (I) Immunofluorescence staining of iPSC-MKs for polymodified tubulin, axonemal dynein, and kinesin-1 show the distribution of both motors along the length of the proplatelet shaft. (J) In *TUBB1* knock-out iPSC-MKs, no proplatelet extensions are formed and a significant reduction in the co-localisation of dynein to polyglutamylated residues is observed (\*  $p = 0.0166$  and \*  $p = 0.0293$  respectively), (L) with no significant change in the co-localisation of kinesin-1 with polyglycylated tubulin.  $n = 3$ , S.D., Two-Way ANOVA with multiple comparisons.

localisation between axonemal dynein and polyglutamylated residues upon platelet spreading (Figure 5 A,B). Interestingly, axonemal dynein is also localised towards the leading edge of platelets when spread on fibrinogen (Figure 5A). This data suggests that the increased polyglutamylation of the marginal band observed on platelet spreading drives an outward movement of axonemal dynein. To confirm the role of axonemal dynein specifically in this process, we also stained spreading platelets for cytoplasmic dynein and observe a central distribution, suggesting an alternative role for cytoplasmic dynein in platelets (Figure S4).

To confirm that the loss of co-localisation observed was specific to polyglutamylated residues, we co-stained resting and spread platelets (fibrinogen and collagen) for both polyglutamylated and polyglycylated tubulin and compared their co-localisation with dynein and kinesin-1, a motor protein recently reported to be important in platelet secretion (33). We found that while in both fibrinogen and collagen spread platelets a leading edge distribution of axonemal dynein is evident (Figure 5) which

239 poorly co-localises with polyglutamylated tubulin, there is no particular spatial relationship between polyglycylated tubulin  
240 and axonemal dynein (Figure 5 C,D,E). A significant decrease in co-localisation is observed in both the fibrinogen and collagen  
241 spread cells (Figure 5 E, H).

242 Interestingly, kinesin-1 is evident throughout the spread platelet, and while there is a significant decrease in the co-localisation  
243 of this motor with polyglutamylated tubulin, there is no change in co-localisation between the polyglycylated residues and  
244 kinesin-1 (Figure 5 F,G,H). This data suggests that polyglutamylated tubulin accelerates motor protein motility as previously  
245 described *in vitro* assays, while polyglycation potentially acts as a 'braking' mechanism.

246 In proplatelet extensions axonemal dynein and kinesin-1 are both evident along the length of the proplatelet shaft (Figure 5 I).  
247 A mechanism of dynein mediated sliding has been reported as the driver of proplatelet elongation, however the original work  
248 cites cytoplasmic dynein as the mediator of this effect(32). Evidence of axonemal dynein in both the platelet and the proplatelet  
249 extension suggests that axonemal dynein likely plays a role in this process. *TUBB1* knock-out cells show no proplatelet  
250 formation, and a significant reduction in the colocalisation of dynein with polyglutamylated residues when compared to wild  
251 type iPSC-MKs (Figure 5K).

## 252 Discussion

253 Platelets and their progenitor cells, megakaryocytes, are a unique model for the study of the tubulin code. Like other specialist  
254 cells, they both express a lineage restricted isoform of  $\beta$  tubulin (*TUBB1*) which is linked to disease pathologies when lost  
255 (inherited macrothrombocytopenias)(5, 18–20). However, unlike other specialist cells which exemplify the tubulin code, MKs  
256 and platelets execute markedly different functions despite their shared  $\beta$ 1 tubulin. MKs are the largest cell of the bone marrow,  
257 typified by a lobed, polyploid nucleus and the generation of long proplatelet extensions into the bone marrow sinusoids for  
258 the generation of platelets. Conversely platelets themselves are anucleate and the smallest circulating component of peripheral  
259 blood, classically involved in haemostasis and thrombosis, but with a myriad of other roles in wound healing, inflammation, and  
260 cancer progression. A key question is therefore how *TUBB1*, restricted to both cell types, helps these cells achieve markedly  
261 different morphologies and functions. We hypothesised that a system of polymodification (polyglutamylation and polyglycy-  
262 lation) targeting the glutamate rich C-terminus of this  $\beta$  tubulin isoform, analogous to similar post-translational modifications  
263 demonstrated in cilia and neuronal cells, is a likely mechanism by which the interactions of  $\beta$ 1 tubulin with key motors are  
264 regulated in both MKs and platelets.

265 The study of this system is complicated by a lack of human cell lines which phenocopy primary MKs, namely in the generation  
266 of proplatelet extensions. Recent advances in the generation of MKs from iPSCs have allowed for the generation of large  
267 pools of mature CD41/42b+ cells, however few of these approaches have yielded large populations of MKs forming proplatelet  
268 networks equivalent to those produced by murine foetal liver cells (34, 35). In the study of the tubulin code and a system of  
269 post-translational modification, a species specific model is needed due to controversies regarding the functionality of particular  
270 modifying enzymes. TTLL10 for example, has both been reported as functionally redundant in humans by Rogowski *et al.*, and  
271 as an 'elongase' requiring the expression of an initiating enzyme (TTLL3) to enact its function as a polyglycylase (25, 28, 36).  
272 Therefore in this work we adapt an existing method of directed differentiation to produce large, proplatelet producing samples  
273 of iPSC-MKs for extensive immunfluorescence analysis of polymodifications and their association with motor proteins.

274 We report a system by which mature, CD42b+ iPSC-MKs demonstrate both polyglutamylation and polyglycylation. We do not  
275 observe any cells with proplatelet extensions lacking these polymodifications. Interestingly, we observe a markedly different  
276 distribution of these PTMs in the resting platelet, where polyglycylation is reduced and polyglutamylation is partially co-  
277 localised to the marginal band. On platelet activation, we observe a marked increase of polyglutamylation specific to the  
278 marginal band. In iPSC-MKs with CRISPR knock-out *TUBB1*, we see a complete loss of proplatelet formation and lose the  
279 distinct re-organisation of polyglutamylated and polyglycylated tubulin around the periphery of MKs as seen in wild type cells.  
280 MK proplatelet extensions are known to be driven by a system of dynein mediated microtubule sliding, while the marginal  
281 band in a resting platelet has been shown to be maintained by the antagonistic movement of dynein and kinesin (13, 14, 32).  
282 Interestingly, polyglutamylation has been reported as a mechanism of altering motor protein processivity, with *in vitro* assays  
283 suggesting that polyglutamylation of  $\beta$  tubulin isoforms like *TUBB1* and *TUBB3* accelerates these motors (29). We show

284 a significant effect of polyglutamylation on the spatial localisation of dynein and kinesin, one which is not evidenced by  
285 polyglycylated residues, supporting *in vitro* assays which suggest that polyglutamylation is an accelerator of motor proteins.  
286 As both polyglutamylation and polyglycylation target the same substrate (a tubulin tail glutamate residue), it is likely that  
287 the competitive modification of these residues allows for the tight regulation of motor protein motility needed for proplatelet  
288 elongation. Interestingly, the re-distribution of platelet polyglutamylation to the marginal band on platelet activation suggests  
289 that this is the mechanism by which the delicate balance of antagonistic motor protein function required to maintain the marginal  
290 band is disrupted.  
291 This system of competitive polymodification is analogous to the post-translational modification of ciliated cells, and so we  
292 reasoned that axonemal dynein, an isoform of the motor exclusive to axonemes, may play a role in both platelet formation  
293 and activation (6, 37, 38). We find evidence of axonemal dynein on both proplatelet extensions and at the leading edge of  
294 spreading platelets. To our knowledge this is the first evidence of a functional role of axonemal dynein outside of classical  
295 ciliated structures. In our *TUBB1* knock-out MKs, we observe a decrease in the colocalisation of dynein to polyglutamylated  
296 tubulin, suggesting that the loss of proplatelet formation observed in these cells is due to a dysregulation of the dynein-mediated  
297 microtubule sliding known to drive the elongation of the proplatelet shaft (32).  
298 Our data suggests a tightly regulated, reversible system of polymodification which must be mediated by the cell specific ex-  
299 pression of TTLLs and CCPs. Our expression profiles show a number of TTLLs and CCPs are expressed by MKs, while  
300 only the polyglutamylase TTLL7 is expressed by platelets, consistent with our finding that in the platelet activation results in  
301 polyglutamylation of the marginal band, but no change in polyglycylation. In MKs we find an increase in expression of two  
302 TTLLs known to be involved in glycation - the initiase TTLL3 and the elongase TTLL10. As previously mentioned, TTLL10  
303 is the source of some controversy in the field, with reports suggesting the acquisition of a mutation in humans which renders the  
304 enzyme non-functional. Our findings support a role of TTLL10 as a polyglycylase on co-expression with TTLL3 as reported  
305 by Ikegami *et al.* in cell lines through co-transfection experiments.  
306 In mice with a variant of the deglutamylase CCP1, an increase in polyglutamylation results in the degeneration of photore-  
307 ceptors in the retina(39). A series of human mutations in the deglutamylase CCP5 have been reported in patients with visual  
308 impairments(40, 41). A loss of glycation has similarly been reported to affect ciliary function and length in mice, and a loss  
309 of this PTM in photoreceptors results in ciliary shortening and subsequent retinal degeneration in mouse models(8, 42). A  
310 knock-out model of TTLL3 results in a loss of glycation and the development of tumours in the colon(43).  
311 In the absence of established TTLL and *TUBB1* specific inhibitors, the role of the PTM of *TUBB1* in human physiology is best  
312 understood by disease models, and much of our current understanding of the tubulin code is derived from correlating the loss  
313 of PTMs with human pathologies (5). We identify two unrelated families with C-terminally oriented *TUBB1* variants, both  
314 presenting with macrothrombocytopenia and supporting a report from Fiore *et al.* suggesting that the loss of the C-terminus is  
315 causative of the disease.  
316 TTLLs are generally, ubiquitously expressed and extensively required for the development of neuronal, retinal, and ciliated  
317 cells. For the first time, we identify 3 unrelated families with *TTLL10* variants which result in an increase in platelet volume  
318 and an established history of bleeding and provides an invaluable insight to the potential role of polyglycylation in the context of  
319 platelet production and function. Our data shows that both TTLL3 and TTLL10 are expressed in platelet producing MKs. Our  
320 patient cohort do not lose TTLL3 function, and as such the action of TTLL3 as an initiase will occupy glutamate residues which  
321 would otherwise be polyglutamylated. In these patients we likely see a loss of polyglycylation, but no co-incident increase in  
322 polyglutamylation due to the action of the initiase (TTLL3). As polyglutamylation and monoglycylation are unaffected, platelet  
323 counts (and production) are normal, however, affected individuals appear to have an increased platelet volume and bleeding,  
324 suggesting a role for the extended glycine tail in regulating platelet size, with a downstream effect on the ability of platelets to  
325 prevent bleeding.

## 326 **Conclusions**

327 The 'tubulin code' posits that a tightly regulated system of post-translational modification as well as the lineage restricted  
328 expression of tubulin isoforms is required to drive unique cellular behaviours. This has been shown through both human

329 disease states and mouse models which demonstrate that the loss of cell specific isoforms or particular regulatory enzymes can  
330 result in a range of neuronal dysfunctions, ciliopathies, abnormal spermatogenesis (or sperm function), and platelet defects. The  
331 loss of *TUBB1* has been established as causative of macrothrombocytopenias, however the mechanisms by which  $\beta$ 1 tubulin  
332 achieves the distinctive morphologies and functions of both MKs and platelets remains elusive.

333 Here we report a tightly regulated expression of glutamylating and glycyllating enzymes through platelet production which  
334 drives the polyglutamylated and polyglycylated of MKs (Figure 6). These modifications are reduced in the terminal platelet  
335 which only expresses the polyglutamylase *TTLL7*, and on activation the marginal band becomes heavily polyglutamylated to  
336 drive motor protein mediated shape change. We show a role for axonemal dynein in proplatelet extension and platelet spreading,  
337 and report novel variants of *TTLL10* which result in bleeding through the loss of its' role as a polyglycylase. Ultimately the  
338 role of this system of polymodification is to fine tune the motility of motor proteins in both the MK and the platelet, allowing  
339 both cell types to achieve their unique functions.

340 This work supports the paradigm of a 'tubulin code', and suggests that there is likely a complex regulatory system upstream of  
341 *TTLLs* and *CCPs* within an MK and a platelet which drives these PTMs.

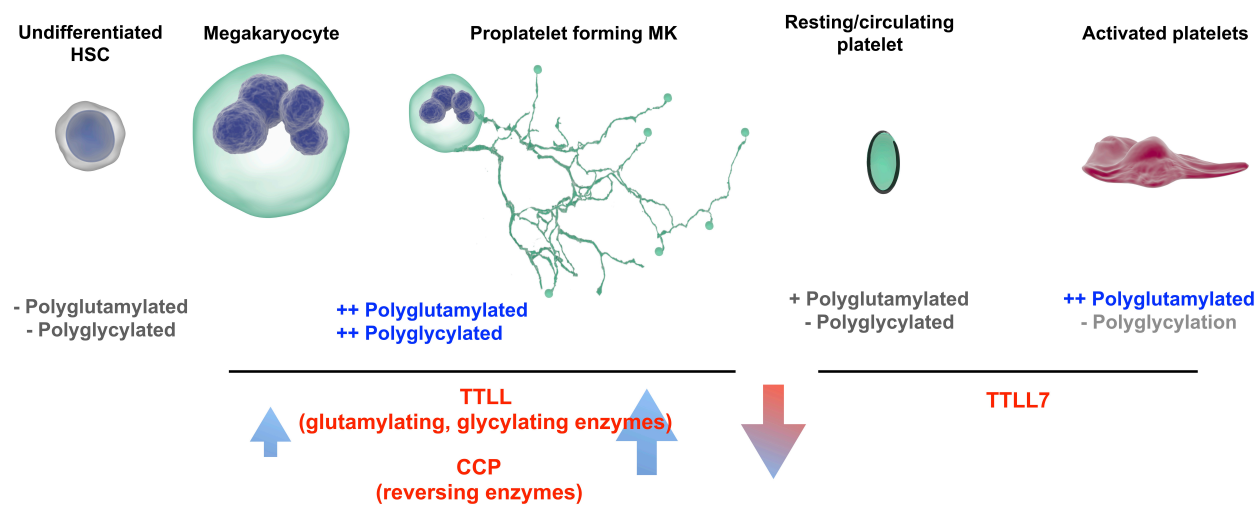


**Fig. 6. A system of competitive polymodification of *TUBB1* driven by the expression of TTLL and CCP enzymes is required for platelet production and function.** We observe a system by which as iPSC-MKs mature and express *TUBB1*, they acquire both polyglutamylated and polyglycylated tubulin which co-incides with an increase in the expression of glutamylating and glycyllating TTLLs and reversing CCPs. A resting platelet is partially polyglutamylated, and on activation the marginal band is polyglutamylated to drive shape change and spreading through the action of *TTLL7*.

## 342 Materials and Methods

343 **Platelet preparation.** Whole blood was obtained for each experiment from healthy volunteers under the University of Birmingham's ERN 11-0175 license 'The regulation of activation of platelets'. Volumes of 25 mL were drawn from volunteers into  
344 sodium citrate. PRP (platelet-rich plasma) was generated by centrifugation of samples for 20 minutes at 200g. PRP was further  
345 spun to isolate platelets by centrifugation at 1,000g for 10 minutes with prostacyclin (0.1  $\mu$ g/mL) and ACD. The resulting pellet  
346 was suspended in Tyrode's buffer prepared fresh, and pre-warmed at 37°C (5mM glucose, 1mM MgCl<sub>2</sub>, 20mM HEPES, 12mM  
347 NaHCO<sub>3</sub>, 2.9 mM KCl, 0.34mM Na<sub>2</sub>HPO<sub>4</sub>, 129mM NaCl to a pH of 7.3). This suspension was spun again at 1,000g with  
348 prostacyclin at the same concentration before re-suspended to a final concentration of 2 x 10<sup>8</sup>/mL. Platelets were left to rest for  
349 30 minutes at room temperature before any further processing or treatment.

351 **Platelet spreading.** Resting platelets were fixed by preparing platelets at a concentration of 4 x 10<sup>7</sup>/mL and mixing with equal  
352 volumes of 10% neutral buffered Formalin in a 15mL falcon tube. This mixture was inverted gently to mix the sample, and  
353 left to incubate for 5 minutes before subsequently adding 300 $\mu$ L of the resulting fixed, resting platelets to coverslips coated in  
354 Poly-L-Lysine (Sigma). Cells were then spun down at 200g for 10 minutes.

355 Spreading was performed on human fibrinogen (Plasminogen, von Willebrand Factor and Fibronectin depleted - Enzyme Re-  
356 search Laboratories) and Horm collagen (Takeda). Coverslips were coated overnight at a concentration of 100  $\mu$ g and 10  $\mu$ g/mL  
357 (fibrinogen and collagen) respectively, before blocking for 1 hour in denatured fatty acid free 1% BSA (Life Technologies).  
358 Finally coverslips were washed once with PBS before the addition of platelets. Unless otherwise stated (as in the time course  
359 experiment), platelets were spread for 45 minutes at 37°C. Fixation for spread platelets was performed in formalin as for resting  
360 platelets for 10 minutes.

361 **Immunofluorescence.** After fixation platelets were washed twice with PBS before incubation in 0.1% Triton X-100 for 5  
362 minutes. The subsequently permeabilised cells were washed twice with PBS before blocking in 2% Goat serum (Life Tech-  
363 nologies) and 1% BSA (Sigma).

364 Fixed, permeabilised, and blocked cells were then incubated with primary antibodies at a concentration of 1:500 unless other-  
365 wise stated. The following antibodies were used for experiments in this work: polyglutamylated tubulin (mouse monoclonal  
366 antibody, clone B3 T9822, Sigma), pan-polyglycylated antibody (mouse monoclonal antibody, AXO49, MABS276 Milli-  
367 pore), monoglycylated antibody (AXO 962 mouse monoclonal MABS277, EMD Millipore), kinesin-1 (rabbit monoclonal to  
368 KIF1B ab 167429, abcam), axonemal dynein,  $\beta$  tubulin (Rabbit polyclonal PA5-16863), tyrosinated tubulin (rabbit monoclonal  
369 antibody, clone YL1/2, MAB1864, EMD Millipore), acetylated tubulin (Lys40, 6-11B-1, mouse monoclonal antibody, Cell  
370 Signalling Technology). DNAL1 antibody (PA5-30643 Invitrogen).

371 After a 1 hour incubation in the relevant mix of primary antibodies. Cells were washed twice with PBS before incubation in  
372 secondary antibodies (Alexa-568-phalloidin, anti-rabbit Alexa-647, anti-mouse Alexa-588 (Life Technologies) for one hour at  
373 a dilution of 1:300 in PBS.

374 **Stem Cell Culture.** Gibco human episomal induced pluripotent stem cell line was purchased from Thermo Scientific and  
375 cultured on Geltrex basement membrane in StemFlex medium (Thermo Scientific).

376 Routine passaging was performed using EDTA (Sigma), with single cell seeding performed for transfection and attempted  
377 clonal isolation through the use of TrypLE (Thermo Scientific). Briefly, cells were washed twice with PBS and once with either  
378 EDTA (for clump passaging) or TrypLE (for single cell) before incubation in 1mL relevant detachment media for 3 minutes at  
379 37°C.

380 For clump passaging, EDTA was removed and 1mL of StemFlex added. Cells were detached by triurting media onto the  
381 bottom of the well and subsequently adding the required volume to fresh media (in a new, GelTrex coated plate).

382 For single cell seeding, TrypLE was diluted in 2mL StemFlex and the solution added to a 15mL falcon tube for centrifugation  
383 at 200g for 4 minutes. The supernatant was then discarded and the cell pellet resuspended in the required volume.

384 **iPSC MK differentiation.** iPSC differentiation to mature, proplatelet forming megakaryocytes was performed using a protocol  
385 based on work published by Feng *et al.* (35). To summarise, cells were detached by clump passaging and seeded on dishes coated  
386 with Collagen Type IV (Advanced Biomatrix) at 5  $\mu$ g/cm<sup>2</sup>. Cells were seeded overnight with RevitaCell (Life Technologies)  
387 to support survival on the new basement substrate. To begin the protocol cells were washed twice and incubated in phase I  
388 medium comprised of APELII medium (Stem Cell Technologies) supplemented with BMP-4 (Thermo Scientific), FGF- $\beta$ , and  
389 VEGF (Stem Cell Technologies) at 50ng/mL each. Cells were incubated at 5% oxygen for the first four days of the protocol  
390 before being placed in a standard cell culture incubator for a further two days in freshly made phase I medium.

391 At day 6 of the protocol cells were incubated in phase II media comprised of APELII, TPO (25 ng/mL), SCF (25 ng/mL), Flt-3  
392 (25ng/mL), Interleukin-3 (10ng/mL), Interleukin-6 (10 ng/mL) and Heparin (5 U/mL) (all supplied by Stem Cell Technologies).

393 Each day in phase II media suspension cells were spun down at 400g for 5 minutes and frozen in 10% FBS/DMSO. After  
394 5 days of collection, all frozen cells were thawed for terminal differentiation. Terminal differentiation was performed by  
395 incubating cells in StemSpan II with heparin (5U/mL) and Stem Cell Technologies Megakaryocyte Expansion supplement on  
396 low attachment dishes (Corning).

397 **RNP Complexes.** The IDT Alt-R®RNP system was used to target and knock-out *TUBB1*. crRNAs were ordered at 2nmol and  
398 resuspended in 20 $\mu$ L TE buffer (IDT) for a final concentration of 100 $\mu$ M. Atto-555 labelled tracrRNAs were ordered at 5nmol  
399 and resuspended in a volume of 50 $\mu$ L for a final concentration of 100 $\mu$ M.

400 To prepare small guide RNAs (sgRNA), equimolar ratios of both crRNA and tracrRNA were mixed with Nuclease Free Duplex  
401 Buffer (IDT). This mix was then incubated at 95°C for 5 minutes before allowing the reaction mix to cool at -1°C/second to  
402 25°C. This mix was then spun down and complexed with either HiFi Cas9 V3 (1081058 - IDT) or Cas9 R10A nickase (1081063  
403 - IDT) purified Alt-R®.

404 Cas9 protein was diluted to 6 $\mu$ g per transfection and incubated with an equal volume of annealed sgRNA. This mix was left for  
405 30 minutes at room temperature to form complete and stable RNP complexes.

406 **Stem Cell Transfection.** iPSC transfection was performed using Lipofectamine Stem (Life Technologies) according to man-  
407 ufacturer instructions. Briefly, iPSC were seeded on 24 well dishes coated with Geltrex at 50,000 cells per well. After an  
408 overnight incubation in StemFlex with RevitaCell, cells were washed twice with PBS and once with OptiMem before incubation  
409 in OptiMem with RevitaCell.

410 RNP complexes were prepared as described in section A and resuspended in 25 $\mu$ L OptiMem per reaction. A Lipofectamine  
411 Stem master mix was prepared using 25 $\mu$ L OptiMem and 2 $\mu$ L Lipofectamine STEM per reaction (4 $\mu$ L if a donor template is  
412 included). Equal volumes of both Lipofectamine and RNP mix were incubated to form lipofection complexes over a 10 minute  
413 incubation at room temperature. The final transfection mix was added to cells in OptiMem and left for 4 hours before the  
414 addition of StemFlex medium (and any relevant small molecules).

415 Measurement of iPSC transfection efficiency after treatment with Lipofectamine STEM and IDT RNP complexes was per-  
416 formed using manual cell counting in Evos acquired images (Phase contrast and fluorescence).

417 **Microscopy.** Images were acquired using an Axio Observer 7 inverted epifluorescence microscope (Carl Zeiss) with Definite  
418 Focus 2 autofocus, 63x 1.4 NA oil immersion objective lens, Colibri 7 LED illumination source, Hammamatsu Flash 4 V2  
419 sCMOS camera, Filter sets 38, 45HQ and 50 for Alexa488, Alexa568 and Alexa647 respectively and DIC optics. LED power  
420 and exposure time were chosen as appropriate for each set of samples but kept the same within each experiment. Using Zen  
421 2.3 Pro software, five images were taken per replicate, either as individual planes (spread platelets) or representative Z-stacks  
422 (resting platelets).

423 **Image and statistical analysis.** Statistical analysis was performed using GraphPad PRISM 7. Image analysis was performed  
424 using a customed workflow. Briefly, the actin channel from resting and spread platelet images was used to train Ilastik pixel  
425 classifiers (approximately 6 images per condition) for segmentation based on this channel. This was incorporated into a KN-  
426 IME workflow which would run images through the classifier to generated segmented binaries in which co-localisation and  
427 fluorescence intensity statistics were calculated (44, 45). For the data presented in this manuscript,  $M1_{diff}$  (a corrected Man-  
428 der's co-efficient to channel 1) was used to determine the co-localisation of PTMs to tubulin, and an  $M2_{diff}$  value (corrected  
429 Mander's co-efficient to channel 2) was used to calculate the co-localisation of motor proteins to PTMs of interest (46).

430 **Quantitative Real Time PCR (qRT-PCR).** To determine whether the 13 mammalian TTLLs and 6 CCPs were expressed in  
431 iPSC-MKs at the different stages of differentiation (day 1, day 5 and day 5 +heparin) a qRT-PCR panel was developed using  
432 TaqMan technology and an ABI 7900 HT analyser (Applied Biosystems, Warrington, UK). RNA samples were isolated and  
433 reverse-transcribed and amplified with the relevant primers using SYBR-Green based technology (Power SYBR(r) Master Mix,  
434 Life Technologies). Total RNA was extracted from iPSC cells using the NucleoSpin RNA kit (Machery-Nagel) and cDNA was  
435 synthesized using the High-Capacity cDNA Reverse Transcription Kit (Life Technologies). qRT-PCR was performed on all  
436 the TTLL/CCP fragments generated from primers designed in supplementary figure 5 and the housekeeping control GAPDH  
437 (GAPDHFOR 5' – GAAGGTGAAGTCGGAGT – 3' and GAPDHREV 5'GAAGATGGTATGGGATTTC – 3').  
438 Each reaction was set up in triplicate including a non-template control. Expression was analysed using the CT method us-  
439 ing D1 undifferentiated cells as a control. A full list of primer sequences has been uploaded as figure S5.

440 **TUBB1 Homology Modelling.** Homology models of TUBB1 WT and mutations were made using SWISS MODEL software  
441 (47–50), using the solved TUBB3 heterodimer as a template (PDB: 5IJ0 (51)). TUBB1 and TUBB3 share approximately 80%  
442 sequence identity, and the model created corresponds to residues 1–425 of TUBB1.

443 **ACKNOWLEDGEMENTS**

444 We thank the families for providing samples and our clinical and laboratory colleagues for their help. This work was supported by the British Heart Foundation (PG/13/36/30275;  
445 FS/13/70/30521; FS/15/18/31317). The authors would like to thank the TechHub and COMPARE Core facilities at the University of Birmingham. We thank Professor Steve  
446 Watson for his ongoing support and invaluable mentorship.

447 **Bibliography**

1. Sudarshan Gadadhar, Satish Bodakuntla, Kathiresan Natarajan, and Carsten Janke. The tubulin code at a glance. *J Cell Sci*, 130(8):1347–1353, Apr 2017. doi: 10.1242/jcs.199471.
2. Sudarshan Gadadhar, Hala Dadi, Satish Bodakuntla, Anne Schnitzler, Ivan Bièche, Filippo Rusconi, and Carsten Janke. Tubulin glyylation controls primary cilia length. *J Cell Biol*, 216(9):2701–2713, 09 2017. doi: 10.1083/jcb.201612050.
3. Sudarshan Gadadhar, Satish Bodakuntla, Kathiresan Natarajan, and Carsten Janke. The tubulin code at a glance. *J Cell Sci*, 130(8):1347–1353, 04 2017. doi: 10.1242/jcs.199471.
4. Richard F Lidueña. A hypothesis on the origin and evolution of tubulin. *Int Rev Cell Mol Biol*, 302:41–185, 2013. doi: 10.1016/B978-0-12-407699-0.00002-9.
5. Maria M Magiera, Puja Singh, and Carsten Janke. Snapshot: Functions of tubulin posttranslational modifications. *Cell*, 173(6):1552–1552.e1, May 2018. doi: 10.1016/j.cell.2018.05.032.
6. Dorota Włoga, Ewa Joachimiak, Panagiota Louka, and Jacek Gaertig. Posttranslational modifications of tubulin and cilia. *Cold Spring Harb Perspect Biol*, 9(6), Jun 2017. doi: 10.1101/cshperspect.a028159.
7. Jeremy F Reiter and Michel R Leroux. Genes and molecular pathways underpinning ciliopathies. *Nat Rev Mol Cell Biol*, 18(9):533–547, Sep 2017. doi: 10.1038/nrm.2017.60.
8. Montserrat Bosch Grau, Christel Masson, Sudarshan Gadadhar, Cecilia Rocha, Olivia Tort, Patricia Marques Sousa, Sophie Vacher, Ivan Bieche, and Carsten Janke. Alterations in the balance of tubulin glyylation and glutamylation in photoreceptors leads to retinal degeneration. *J Cell Sci*, 130(5):938–949, Mar 2017. doi: 10.1242/jcs.199091.
9. Koji Ikegami, Showbu Sato, Kenji Nakamura, Lawrence E Ostrowski, and Mitsutoshi Setou. Tubulin polyglutamylation is essential for airway ciliary function through the regulation of beating asymmetry. *Proc Natl Acad Sci U S A*, 107(23):10490–5, Jun 2010. doi: 10.1073/pnas.1002128107.
10. Hui-Yuan Wu, Peng Wei, and James I Morgan. Role of cytosolic carboxypeptidase 5 in neuronal survival and spermatogenesis. *Sci Rep*, 7:41428, 01 2017. doi: 10.1038/srep41428.
11. P Vogel, G Hansen, G Fontenot, and R Read. Tubulin tyrosine ligase-like 1 deficiency results in chronic rhinosinusitis and abnormal development of spermatid flagella in mice. *Vet Pathol*, 47(4):703–12, Jul 2010. doi: 10.1177/0300985810363485.
12. Serge Dmitrieff, Adolfo Alsina, Aastha Mathur, and François J Nédélec. Balance of microtubule stiffness and cortical tension determines the size of blood cells with marginal band across species. *Proc Natl Acad Sci U S A*, 114(17):4418–4423, Apr 2017. doi: 10.1073/pnas.1618041114.
13. Boubou Diagouraga, Alexei Grichine, Arnold Fertin, Jin Wang, Saadi Khochbin, and Karin Sadoul. Motor-driven marginal band coiling promotes cell shape change during platelet activation. *J Cell Biol*, 204(2):177–85, Jan 2014. doi: 10.1083/jcb.201306085.
14. K Sadoul. New explanations for old observations: marginal band coiling during platelet activation. *J Thromb Haemost*, 13(3):333–46, Mar 2015. doi: 10.1111/jth.12819.
15. Natalie S Poulter and Steven G Thomas. Cytoskeletal regulation of platelet formation: Coordination of f-actin and microtubules. *Int J Biochem Cell Biol*, 66:69–74, Sep 2015. doi: 10.1016/j.biocel.2015.07.008.
16. Kellie R Machliss and Joseph E Italiano, Jr. The incredible journey: From megakaryocyte development to platelet formation. *J Cell Biol*, 201(6):785–96, Jun 2013. doi: 10.1083/jcb.201304054.
17. H D Schwer, P Lecine, S Tiwari, J E Italiano, Jr, J H Hartwig, and R A Shivdasani. A lineage-restricted and divergent beta-tubulin isoform is essential for the biogenesis, structure and function of blood platelets. *Curr Biol*, 11(8):579–86, Apr 2001.
18. Shinji Kunishima, Ryoji Kobayashi, Tomohiko J Itoh, Motohiro Hamaguchi, and Hidehiko Saito. Mutation of the beta1-tubulin gene associated with congenital macrothrombocytopenia affecting microtubule assembly. *Blood*, 113(2):458–61, Jan 2009. doi: 10.1182/blood-2008-06-162610.
19. Shinji Kunishima, Satoshi Nishimura, Hidenori Suzuki, Masue Imaizumi, and Hidehiko Saito. Tubb1 mutation disrupting microtubule assembly impairs proplatelet formation and results in congenital macrothrombocytopenia. *Eur J Haematol*, 92(4):276–82, Apr 2014. doi: 10.1111/ehj.12252.
20. M Fiore, C Goulas, and X Pillois. A new mutation in tubb1 associated with thrombocytopenia confirms that c-terminal part of  $\beta$ 1-tubulin plays a role in microtubule assembly. *Clin Genet*, 91(6):924–926, Jun 2017. doi: 10.1111/cge.12879.
21. Sunita Patel-Hett, Jennifer L Richardson, Harald Schulze, Ksenija Drabek, Natasha A Isaac, Karin Hoffmeister, Ramesh A Shivdasani, J Chloë Bulinski, Niels Galjart, John H Hartwig, and Joseph E Italiano, Jr. Visualization of microtubule growth in living platelets reveals a dynamic marginal band with multiple microtubules. *Blood*, 111(9):4605–16, May 2008. doi: 10.1182/blood-2007-10-118844.
22. Kathiresan Natarajan, Sudarshan Gadadhar, Judith Souphron, Maria M Magiera, and Carsten Janke. Molecular interactions between tubulin tails and glutamylases reveal determinants of glutamylation patterns. *EMBO Rep*, 18(6):1013–1026, Jun 2017. doi: 10.15252/embr.201643751.
23. A Wolff, B de Néchaud, D Chillet, H Mazarguil, E Desbruyères, S Audebert, B Eddé, F Gros, and P Denoulet. Distribution of glutamylated alpha and beta-tubulin in mouse tissues using a specific monoclonal antibody, gt335. *Eur J Cell Biol*, 59(2):425–32, Dec 1992.
24. Dorota Włoga, Danielle M Webster, Krzysztof Rogowski, Marie-Hélène Bré, Nicolette Levilliers, Maria Jerka-Dziadosz, Carsten Janke, Scott T Dougan, and Jacek Gaertig. Ttll3 is a tubulin glycine ligase that regulates the assembly of cilia. *Dev Cell*, 16(6):867–76, Jun 2009. doi: 10.1016/j.devcel.2009.04.008.
25. Krzysztof Rogowski, François Juge, Juliette van Dijk, Dorota Włoga, Jean-Marc Strub, Nicolette Levilliers, Daniel Thomas, Marie-Hélène Bré, Alain Van Dorsselaer, Jacek Gaertig, and Carsten Janke. Evolutionary divergence of enzymatic mechanisms for posttranslational polyglcylation. *Cell*, 137(6):1076–87, Jun 2009. doi: 10.1016/j.cell.2009.05.020.
26. Alu Konno, Koji Ikegami, Yoshiyuki Konishi, Hyun-Jeong Yang, Manabu Abe, Maya Yamazaki, Kenji Sakimura, Ikuko Yao, Kogiku Shiba, Kazuo Inaba, and Mitsutoshi Setou. Ttll9-/- mice sperm flagella show shortening of doublet 7, reduction of doublet 5 polyglutamylation and a stall in beating. *J Cell Sci*, 129(14):2757–66, 07 2016. doi: 10.1242/jcs.185983.
27. R J Mullen, E M Eicher, and R L Sidman. Purkinje cell degeneration, a new neurological mutation in the mouse. *Proc Natl Acad Sci U S A*, 73(1):208–12, Jan 1976.
28. Koji Ikegami, Robb L Heier, Midori Taruishi, Hiroshi Takagi, Masahiro Mukai, Shuichi Shimma, Shu Taira, Ken Hatanaka, Nobuhiro Morone, Ikuko Yao, Patrick K Campbell, Shigeki Yuasa, Carsten Janke, Grant R Macgregor, and Mitsutoshi Setou. Loss of alpha-tubulin polyglutamylation in rosa22 mice is associated with abnormal targeting of kif1a and modulated synaptic function. *Proc Natl Acad Sci U S A*, 104(9):3213–8, Feb 2007. doi: 10.1073/pnas.0611547104.
29. Minhajuddin Sirajuddin, Luke M Rice, and Ronald D Vale. Regulation of microtubule motors by tubulin isoatypes and post-translational modifications. *Nat Cell Biol*, 16(4):335–44, Apr 2014. doi: 10.1038/ncb2920.
30. Juliette van Dijk, Guillaume Bompard, Julien Cau, Shinji Kunishima, Gabriel Rabeharivel, Julio Mateos-Langerak, Chantal Cazeveille, Patricia Cavelier, Brigitte Boizet-Bonhoure, Claude Delset, and Nathalie Morin. Microtubule polyglutamylation and acetylation drive microtubule dynamics critical for platelet formation. *BMC Biol*, 16(1):116, 10 2018. doi: 10.1186/s12915-018-0584-6.
31. Koji Ikegami and Mitsutoshi Setou. Ttll10 can perform tubulin glyylation when co-expressed with ttll8. *FEBS Lett*, 583(12):1957–63, Jun 2009. doi: 10.1016/j.febslet.2009.05.003.
32. Markus Bender, Jonathan N Thon, Allen J Ehrlicher, Stephen Wu, Linas Mazutis, Emoke Deschmann, Martha Sola-Visner, Joseph E Italiano, and John H Hartwig. Microtubule sliding drives proplatelet elongation and is dependent on cytoplasmic dynein. *Blood*, 125(5):860–8, Jan 2015. doi: 10.1182/blood-2014-09-600858.
33. Frédéric Adam, Alexandre Kauskot, Mathieu Kurowska, Nicolas Goudin, Isabelle Munoz, Jean-Claude Bordet, Jian-Dong Huang, Marijke Bryckaert, Alain Fischer, Delphine Borgel, Geneviève

504 de Saint Basile, Olivier D Christophe, and Gaël Ménasché. Kinesin-1 is a new actor involved in platelet secretion and thrombus stability. *Arterioscler Thromb Vasc Biol*, 38(5):1037–1051, May 2018.  
505 doi: 10.1161/ATVBAHA.117.310373.

506 34. Thomas Moreau, Amanda L Evans, Louella Vasquez, Marloes R Tijsen, Ying Yan, Matthew W Trotter, Daniel Howard, Maria Colzani, Meera Arumugam, Wing Han Wu, Amanda Dalby, Riina  
507 Lampela, Guenaelle Bouet, Catherine M Hobbs, Dean C Pask, Holly Payne, Tatyana Ponomaryov, Alexander Brill, Nicole Soranzo, Willem H Ouwehand, Roger A Pedersen, and Cedric Ghevaert.  
508 Large-scale production of megakaryocytes from human pluripotent stem cells by chemically defined forward programming. *Nat Commun*, 7:11208, Apr 2016. doi: 10.1038/ncomms11208.

509 35. Qiang Feng, Namrata Shabrani, Jonathan N Thon, Hongguang Huo, Austin Thiel, Kellie R Machlus, KyungHo Kim, Julie Brooks, Feng Li, Chenmei Luo, Erin A Kimbrel, Jiwu Wang, Kwang-Soo Kim,  
510 Joseph Italiano, Jaehyung Cho, Shi-Jiang Lu, and Robert Lanza. Scalable generation of universal platelets from human induced pluripotent stem cells. *Stem Cell Reports*, 3(5):817–31, Nov 2014.  
511 doi: 10.1016/j.stemcr.2014.09.010.

512 36. Sou Nakamura, Naoya Takayama, Shinji Hirata, Hideya Seo, Hiroshi Endo, Kiyosumi Ochi, Ken-ichi Fujita, Tomo Koike, Ken-ichi Harimoto, Takeaki Dohda, Akira Watanabe, Keisuke Okita, Nobuyasu  
513 Takahashi, Akira Sawaguchi, Shinya Yamanaka, Hiromitsu Nakauchi, Satoshi Nishimura, and Koji Eto. Expandable megakaryocyte cell lines enable clinically applicable generation of platelets from  
514 human induced pluripotent stem cells. *Cell Stem Cell*, 14(4):535–48, Apr 2014. doi: 10.1016/j.stem.2014.01.011.

515 37. Robert O'Hagan, Malan Silva, Ken C Q Nguyen, Winnie Zhang, Sebastian Bellotti, Yasmin H Ramadan, David H Hall, and Maureen M Barr. Glutamylate regulates transport, specializes function,  
516 and sculpts the structure of cilia. *Curr Biol*, 27(22):3430–3441.e6, Nov 2017. doi: 10.1016/j.cub.2017.09.066.

517 38. Dorota Wloda, Drashti Dave, Jennifer Meagley, Krzysztof Rogowski, Maria Jerka-Dziadosz, and Jacek Gaertig. Hyperglutamylate of tubulin can either stabilize or destabilize microtubules in the  
518 same cell. *Eukaryot Cell*, 9(1):184–93, Jan 2010. doi: 10.1128/EC.00176-09.

519 39. Miguel Marchena, Juan Lara, José Aijón, Francisco Germain, Pedro de la Villa, and Almudena Velasco. The retina of the pcd/pcd mouse as a model of photoreceptor degeneration. a structural and  
520 functional study. *Exp Eye Res*, 93(5):607–17, Nov 2011. doi: 10.1016/j.exer.2011.07.010.

521 40. Galuh D N Astuti, Gavin Arno, Sarah Hull, Laurence Pierrache, Hanka Venselaar, Keren Cars, F Lucy Raymond, Rob W J Collin, Sultana M H Faradz, L Ingeborgh van den Born, Andrew R Webster,  
522 and Frans P M Cremers. Mutations in agbl5, encoding  $\alpha$ -tubulin deglutamylase, are associated with autosomal recessive retinitis pigmentosa. *Invest Ophthalmol Vis Sci*, 57(14):6180–6187, Nov  
523 2016. doi: 10.1167/iovs.16-20148.

524 41. Sandra E Branham, Sara J Wright, Aaron Reba, and C Randal Linder. Genome-wide association study of arabidopsis thaliana identifies determinants of natural variation in seed oil composition. *J  
525 Hered*, 107(3):248–56, 05 2016. doi: 10.1093/jhered/esv100.

526 42. Montserrat Bosch Grau, Christel Masson, Sudarshan Gadadhar, Cecilia Rocha, Olivia Tort, Patricia Marques Sousa, Sophie Vacher, Ivan Bieche, and Carsten Janke. Alterations in the balance of  
527 tubulin glycation and glutamylate in photoreceptors leads to retinal degeneration. *J Cell Sci*, 130(5):938–949, 03 2017. doi: 10.1242/jcs.199091.

528 43. Cecilia Rocha, Laura Papon, Wulfran Cacheux, Patricia Marques Sousa, Valeria Lascano, Olivia Tort, Tiziana Giordano, Sophie Vacher, Benedicte Lemmers, Pascale Mariani, Didier Meseure,  
529 Jan Paul Medema, Ivan Bièche, Michael Hahne, and Carsten Janke. Tubulin glycylases are required for primary cilia, control of cell proliferation and tumor development in colon. *EMBO J*, 33(19):  
530 2247–60, Oct 2014. doi: 10.15252/embj.201488466.

531 44. M R Berthold, N Cebron, F Dill, T Gabriele, Kötter R, T T, Meinl, P Ohl, K Thiel, and B Wiswedel. Knime-the konstanz information miner: version 2.0 and beyond. *AcM SIGKDD explorations  
532 Newsletter*, 11(1):26–31, 2009.

533 45. C Sommer, C Strahle, F Kothe, and Hamprecht F A. ilastik: Interactive learning and segmentation toolkit. *Eighth IEEE International Symposium on Biomedical Imaging (ISBI)*, Proceedings:  
534 230–233, 2011.

535 46. John H McDonald and Kenneth W Dunn. Statistical tests for measures of colocalization in biological microscopy. *J Microsc*, 252(3):295–302, Dec 2013. doi: 10.1111/jmi.12093.

536 47. Andrew Waterhouse, Martino Bertoni, Stefan Bienert, Gabriel Studer, Gerardo Tauriello, Rafal Gumienny, Florian T Heer, Tjaart A P de Beer, Christine Rempfer, Lorenza Bordoli, Rosalba Lepore, and  
537 Torsten Schwede. SWISS-MODEL: homology modelling of protein structures and complexes. *Nucleic Acids Research*, 46(W1):W296–W303, 05 2018. ISSN 0305-1048. doi: 10.1093/nar/gky427.

538 48. Stefan Bienert, Andrew Waterhouse, Tjaart A. P. de Beer, Gerardo Tauriello, Gabriel Studer, Lorenza Bordoli, and Torsten Schwede. The SWISS-MODEL Repository—new features and functionality.  
539 *Nucleic Acids Research*, 45(D1):D313–D319, 11 2016. ISSN 0305-1048. doi: 10.1093/nar/gkw1132.

540 49. Nicolas Guex, Manuel C Peitsch, and Torsten Schwede. Automated comparative protein structure modeling with swiss-model and swiss-pdbviewer: A historical perspective. *Electrophoresis*, 30  
541 (S1):S162–S173, 2009. ISSN 0173-0835.

542 50. Pascal Benkert, Marco Biasini, and Torsten Schwede. Toward the estimation of the absolute quality of individual protein structure models. *Bioinformatics*, 27(3):343–350, 12 2010. ISSN 1367-4803.  
543 doi: 10.1093/bioinformatics/btq662.

544 51. Shih-Chieh Ti, Melissa C. Pamula, Stuart C. Howes, Christian Duellberg, Nicholas I. Cade, Ralph E. Kleiner, Scott Forth, Thomas Surrey, Eva Nogales, and Tarun M. Kapoor. Mutations in human  
545 tubulin proximal to the kinesin-binding site alter dynamic instability at microtubule plus- and minus-ends. *Developmental Cell*, 37(1):72 – 84, 2016. ISSN 1534-5807. doi: <https://doi.org/10.1016/j.devcel.2016.03.003>.